Title
Characterization of the chemical signatures of air masses observed during the PEM experiments over the western Pacific

Journal
Journal of Geophysical Research, 104(D13)

ISSN
0148-0227

Authors
Smyth, S
Sandholm, S
Shumaker, B
et al.

Publication Date
1999-07-20

DOI
10.1029/1999jd900115

JOURNAL OF GEOPHYSICAL RESEARCH, VOL. 104, NO. D13, PAGES 16,243–16,254, JULY 20, 1999

Characterization of the chemical signatures of air masses observed during the PEM experiments over the western Pacific

S. Smyth,[1] S. Sandholm,[1] B. Shumaker,[1] W. Mitch,[1] A. Kanvinde,[1] J. Bradshaw,[1] S. Liu,[1] S. McKeen,[2] G. Gregory,[3] B. Anderson,[3] R. Talbot,[4] D. Blake,[5] S. Rowland,[5] E. Browell,[3] M. Fenn,[3] J. Merrill,[6] S. Bachmeier,[7,8] G. Sachse,[3] and J. Collins[3]

Abstract. Extensive observations of tropospheric trace species during the second NASA Global Tropospheric Experiment Western Pacific Exploratory Mission (PEM-West B) in February–March 1994 showed significant seasonal variability in comparison with the first mission (PEM-West A), conducted in September–October 1991. In this study we adopt a previously established analytical method, i.e., the ratio C_2H_2/CO as a measure of the relative degree of atmospheric processing, to elucidate the key similarities and variations between the two missions. In addition, the C_2H_2/CO ratio scheme is combined with the back-trajectory-based and the LIDAR-based air mass classification schemes, respectively, to make in-depth analysis of the seasonal variation between PEM-West A and PEM-West B (hereinafter referred to as PEM-WA and PEM-WB). A large number of compounds, including long-lived NMHCs, CH_4, and CO_2, are, as expected, well correlated with the ratio C_2H_2/CO. In comparison with PEM-WA, a significantly larger range of observed C_2H_2/CO values at the high end for the PEM-WB period indicates that the western Pacific was more impacted by "fresher" source emissions, i.e., faster or more efficient continental outflow. As in the case of PEM-WA, the C_2H_2/CO scheme complements the back-trajectory air mass classification scheme very well. By combining the two schemes, we found that the atmospheric processing in the region is dominated by atmospheric mixing for the trace species analyzed. This PEM-WB wintertime result is similar to that found in PEM-WA for the autumn. In both cases, photochemical reactions are found to play a significant role in determining the background mixing ratios of trace gases, and in this way the two processes are directly related and dependent upon each other. This analysis also indicates that many of the upper tropospheric air masses encountered over the western Pacific during PEM-WB may have had little impact from eastern Asia's continental surface sources. NO_x mixing ratios were significantly enhanced during PEM-WB when compared with PEM-WA, in the upper troposphere's more atmospherically processed air masses. These high levels of NO_x resulted in a substantial amount of photochemical production of O_3. A lack of corresponding enhancements in surface emission tracers strongly implies that in situ atmospheric sources such as lightning are responsible for the enhanced upper tropospheric NO_x. The similarity in NO_x values between the northern (higher air traffic) and southern continental air masses together with the indications of a large seasonal shift suggests that aircraft emissions are not the dominant source. However, photochemical recycling cannot be ruled out as this in situ source of NO_x.

1. Introduction

The Pacific Exploratory Missions (PEM) conducted over the western Pacific under NASA's Global Tropospheric Experiment (GTE) consisted of two primary components of field experiment: PEM-West A and PEM-West B (hereinafter referred to as PEM-WA and PEM-WB). The major goals of the PEM-West campaigns were to characterize the transport and chemistry of the natural and anthropogenic emissions into the northwestern Pacific region. Specific emphasis was on the tropospheric ozone, its precursors, and some sulfur species. PEM-WB complemented the PEM-WA experiment conducted in the autumn (September–October) of 1991 by making similar measurements over the western Pacific during the late winter/early spring (February–March) of 1994 under contrasting meteorological conditions [*Merrill et al.*, 1997]. Plate 1 shows the flight routes of the NASA DC-8 aircraft during the two campaigns. An overview and a summary of the major scientific findings of the PEM-WB campaign are given by *Hoell et al.* [1997].

Several compounds measured on board the DC-8 aircraft during PEM-WA and PEM-WB are good indicators of anthropogenic and/or biogenic emissions from the Asian continent

[1]School of Earth and Atmospheric Sciences, Georgia Institute of Technology, Atlanta.
[2]NOAA, Aeronomy Laboratory, Boulder, Colorado.
[3]NASA Langley Research Center, Hampton, Virginia.
[4]Institute for the Study of Earth, Oceans, and Space, University of New Hampshire, Durham.
[5]Department of Chemistry, University of California at Irvine.
[6]Center for Atmospheric Chemistry Studies, Graduate School of Oceanography, University of Rhode Island, Narragansett.
[7]Science Applications International Corporation, Hampton, Virginia.
[8]Now at Department of Atmospheric, Oceanic and Space Science, University of Wisconsin, Madison.

Paper number 1999JD900115.
0148-0227/99/1999JD900115$09.00

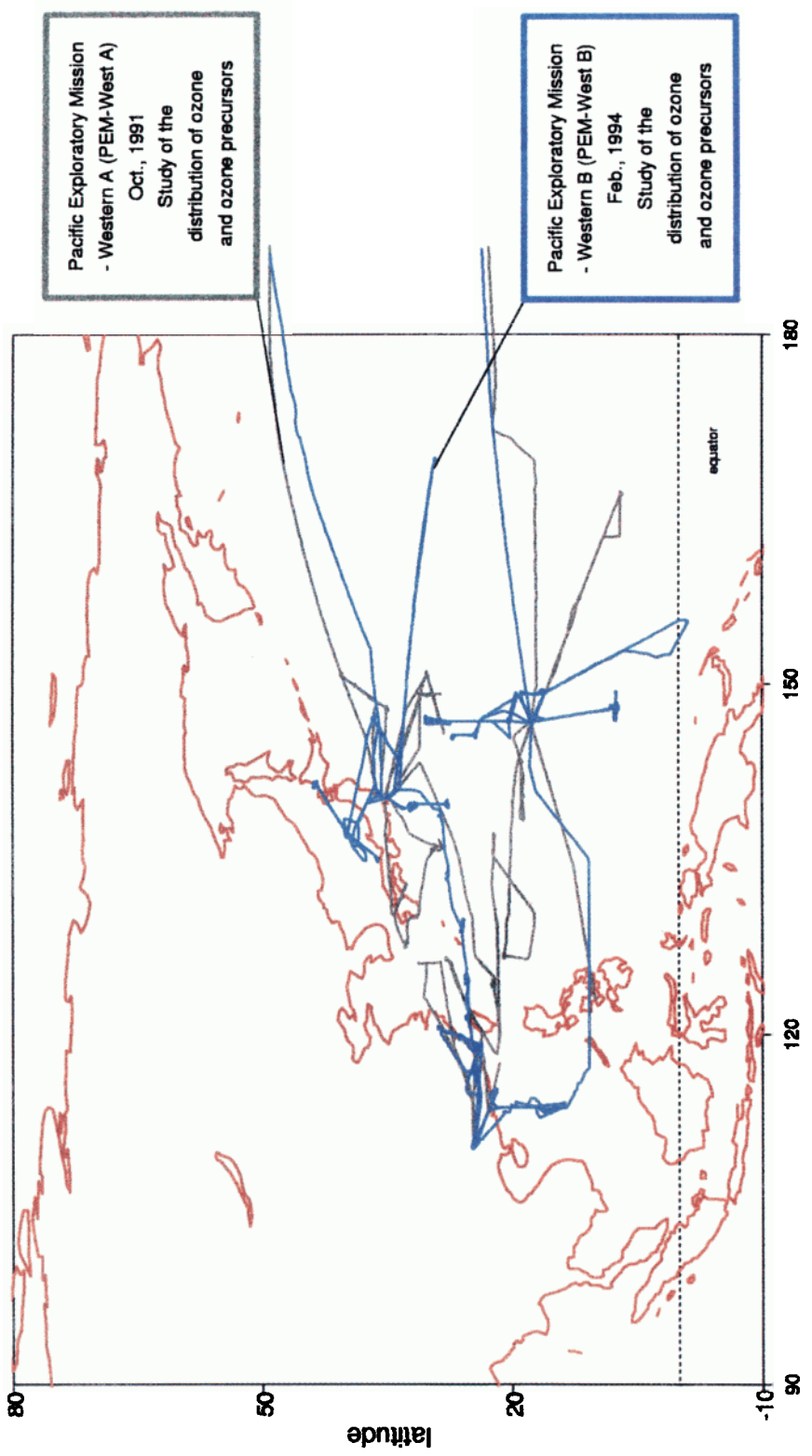

Plate 1. NASA Global Tropospheric Experiment Pacific Exploratory Mission (PEM) West A (gray) and PEM-West B (blue) flight tracks for all flights in the western Pacific region.

(including the Pacific Rim), for example, NMHCs, methane (CH_4), carbon monoxide (CO), carbon dioxide (CO_2), oxides of nitrogen (NO_x = NO + NO_2), and sulfur dioxide (SO_2). Changes in the mixing ratios of these trace species in various air masses observed over the western Pacific are indicative of the degrees of impact of the continental emissions. Among the trace species, NMHCs such as C_2H_6, C_3H_8, and C_2H_2 and CO are particularly useful tracers of continental inputs because they do not have significant oceanic sources and their sinks due to reactions with OH radicals are relatively simple compared with other species such as NO_x and SO_2. In fact, ratios of NMHCs have been used as a method of isolating the chemical loss of NMHCs due to reaction with OH and from that deriving the concentration of OH. The idea behind the method is to use the ratios to cancel the changes of the mixing ratios due to atmospheric mixing and the spatially and temporally inhomogeneous emissions. However, *McKeen and Liu* [1993] have shown that this method cannot effectively remove the influence of atmospheric mixing. Moreover, analysis of the PEM-WA data confirms their conclusion that atmospheric mixing significantly affects the ratio of such compounds [*McKeen et al.*, 1996; *Smyth et al.*, 1996]. In fact, the latter two studies have demonstrated that ratios of compounds emitted from common sources can be used for estimating the relative degree of atmospheric processing due to both atmospheric mixing and photochemical reactions.

Smyth et al. [1996] have successfully used the ratio C_2H_2/CO as a measure of the degree of atmospheric processing of a continental air mass because the dominant chemical sink of both compounds is via reaction with OH and its dominant source is production from combustion. The reaction of C_2H_2 with OH is approximately 3 times faster than that for CO with OH. Thus the C_2H_2/CO ratio decreases with increasing atmospheric processing (which is often, but not necessarily, proportional to the length of time after emissions of C_2H_2 and CO) as the air mass travels away from the source region (e.g., from Asia to the Pacific Ocean). This C_2H_2/CO ratio has been demonstrated to be very valuable in isolating and evaluating the impact of the contributions from combustion sources for remote regions investigated in previous GTE programs [*Sandholm et al.*, 1992, 1994; *Smyth et al.*, 1996]. In addition, for the PEM-WA analysis, *Smyth et al.* [1996] compared the C_2H_2/CO ratio scheme of characterizing air masses to back-trajectory [*Gregory et al.*, 1996; *Talbot et al.*, 1996] and LIDAR [*Browell et al.*, 1996] air mass classification schemes. They found that the C_2H_2/CO ratio scheme was consistent with the other two schemes and thus provided a valuable independent tool for investigating the distributions and budgets of various atmospheric trace species. More important, they found that the C_2H_2/CO ratio scheme (that later on will be referred to as the chemically based air mass classification scheme) complemented the other two schemes effectively and that these schemes could be combined together to become a more powerful tool to analyze and interpret the observations. Therefore, in this study we adopt the same technique of *Smyth et al.* [1996] to analyze and interpret the observations of PEM-WB. The focus of the study will be to characterize the air masses and to investigate the distributions and budgets of trace species. In addition, the results of PEM-WB are compared with those of PEM-WA to elucidate the key similarities and variations between the two missions.

In the next section we give a brief description of meteorological conditions during PEM-WB and compare them with those of PEM-WA. Particular emphasis has been given to characterizing the difference in the continental outflows of the two experiments because the major features of C_2H_2/CO depend critically on the characteristics of the continental outflow. In section 3 we use the C_2H_2/CO ratio as a measure of the degree of atmospheric processing to study the distributions and budgets of a number of key trace species observed during PEM-WB and make comparisons with those of PEM-WA. In sections 4.1 and 4.2 the C_2H_2/CO ratio scheme is combined with the back-trajectory-based and the LIDAR-based air mass classification schemes, respectively, to make an in-depth analysis of the seasonal variation between PEM-WA and PEM-WB. Section 5 gives a summary of the major findings and conclusions.

2. Meteorological Conditions of PEM-West B Versus PEM-West A

The meteorology during February and March 1994 of PEM-WB contrasts sharply with that encountered during PEM-WA (September–October, 1991). From a large-scale perspective the meteorological differences between PEM-WA and PEM-WB can be characterized by the position and strength of the Japan Jet and the location of the Pacific High [*Merrill et al.*, 1997]. During PEM-WA the Japan Jet tends to be weaker and positioned more northerly than during the late winter to early spring (i.e., during PEM-WB). As a result, the PEM-WA study period was characterized by more inflow of marine air into the midlatitudes, accompanied by extensive vertical mixing along a typhoon storm track running roughly parallel with the Asian coast. In the meantime, the continental outflow tended to be limited to north of about 40°N latitude.

In contrast, the PEM-WB period was characterized by enhanced continental outflow throughout the studied region, with an increased number of frontal passages and a pronounced continental enhancement as far south as about 20°N latitude. Thus we expect significantly greater values in both the C_2H_2/CO ratio and the absolute levels of continental trace species during PEM-WB than during PEM-WA. On the other hand, the continental trace species were, in general, limited to below 6 km altitude during PEM-WB, while more active convective activities during PEM-WA transported more pollutants to the upper troposphere and then to the Pacific basin by the westerlies [*Blake et al.*, 1996; *Liu et al.*, 1996]. For example, *Blake et al.* [1997] demonstrated that in both midlatitude (>25°N) and low-latitude (<25°N) regions, the anthropogenic NMHC mixing ratios in the upper troposphere during PEM-WA were discernibly higher than those observed during PEM-WB. This is particularly significant because the mixing ratios of NMHCs in the lower troposphere tend to have seasonal maxima in winter or early spring [e.g., *Singh and Zimmerman* 1992] because of the lower concentration of OH during the winter [*Crawford et al.*, 1997b].

3. Use of C_2H_2/CO to Characterize Trace Species

During PEM-WB the mixing ratios of C_2H_6 and C_3H_8 were correlated with the C_2H_2/CO ratio (Figures 1a and 1b) throughout the range of C_2H_2/CO except at the lowest values, where both C_2H_6 and C_3H_8 tended to approach their background levels (more clearly shown in logarithmic scale in Figures 2b and 2c). The covariance of C_2H_6 and C_3H_8 relative to

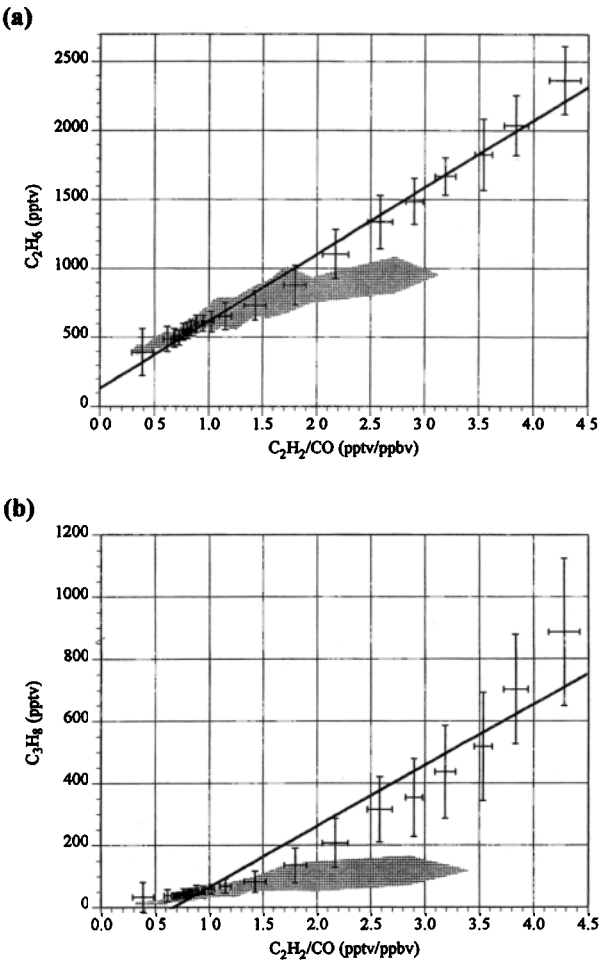

Figure 1. Graph of data for selected trace gases versus the ratio C_2H_2/CO for PEM-West B, where vertical bars indicate $\pm 1\sigma$ about the mean for (a) C_2H_6 and (b) C_3H_8 and where the least squares fit line (thin line) is depicted for those data having C_2H_2/CO ratios between 0.5 and 4.5 pptv/ppbv. The shaded regions represent the entire PEM-West A data set above 2 km within $\pm 1\sigma$. These graphs include all of the PEM-West A and PEM-West B NMHC data except the largest 2% of the mixing ratios, which were omitted because they represent anomalously high mixing ratios measured in small spatial-scale events from isolated emission sources. Each aggregate point contains 5% of the remaining NMHC measurements made during the portion of PEM-West B covering the western and central Pacific at altitudes higher than 2 km.

C_2H_2/CO for the PEM-WB data is similar to that expected for the atmospheric processing of species with similar origins and sinks [*McKeen et al.*, 1996; *Smyth et al.*, 1996]. Although similar trends exist for both PEM-WA and PEM-WB, the late winter data clearly extend the covariance relationship between these two alkanes and the C_2H_2/CO atmospheric processing scale to significantly larger values (i.e., fresher emission). In addition, C_2H_6 and C_3H_8 mixing ratios of PEM-WB are higher than those of PEM-WA for the same value of C_2H_2/CO except near the lowest value. This difference between PEM-WA and PEM-WB is expected due to the larger continental outflow into the western Pacific Basin and smaller chemical loss from reaction with OH during the winter relative to autumn, as discussed in section 1. In contrast, PEM-WB and PEM-WA have similar mixing ratios of C_2H_6 and C_3H_8 at the low end of C_2H_2/CO. This is because the air masses at the low end of C_2H_2/CO are dominated by low-latitude marine air masses which have relatively little seasonal dependence.

Compounds with similar sources and lifetimes should exhibit relationships similar to those observed for C_2H_6 and C_3H_8 with respect to the ratio C_2H_2/CO, i.e., they should exhibit decreasing concentrations with an increasing degree of atmospheric processing. CH_4 and other NMHCs belong to this category. In contrast, compounds with significant noncontinental sources such as in situ atmospheric sources (e.g., photochemical production and oceanic emissions) can deviate from the above relationships because these sources can maintain or even increase the level of the compound as the degree of atmospheric processing of the original continental source increases. This was found to be the case for O_3, NO_x, and NO_y (total reactive nitrogen species) based on our analysis of the PEM-WA data [*Smyth et al.*, 1996]. The noncontinental sources found were photochemical production for O_3 and lightning for NO_x and NO_y.

Figures 2a–2h compare the behavior between the PEM-WB and PEM-WA data using aggregated means ($\pm 1\sigma$) of the PEM-WB data that are separated into altitude bins of 2–7 km and 7–12 km and where the shaded regions represent $\pm 1\sigma$ distribution for all the PEM-WA data from 2 to 12 km. These altitude bins omit the data in the lowest 2 km because of difficulties in interpreting low-altitude back-trajectories (used later). The altitude bins chosen for these two groups were based on the PEM-WA analysis, which indicated that the enhanced mixing ratios associated with the continental outflow primarily occurred in the 2- to 8-km range [*Gregory et al.*, 1996; *Talbot et al.*, 1996]. Thus 7 km was a convenient dividing altitude for the two altitude bins. The same altitude bins are adopted here to facilitate the comparison with results of PEM-WA. Fortunately, as discussed earlier, the bulk of continental outflow during PEM-WB occurred in the lower troposphere (<6 km) [*Blake et al.*, 1997; *Talbot et al.*, 1997], making the comparison more meaningful.

CH_4 and the NMHCs in Figures 2a–2d are correlated with the C_2H_2/CO ratio for both altitude regimes. CH_4 has anthropogenic and biogenic sources, which are predominantly located on the continent, suggesting that its covariance with C_2H_2/CO is an indication of a general colocation of their sources. The anthropogenic compound C_6H_6 also displays a similar trend at larger values but plateaus to a nearly constant nonvarying value in air masses that are more processed (i.e., that have smaller C_2H_2/CO values). On average, CH_4 mixing ratios decreased by 4%, from approximately 1770 to 1700 ppbv, over the range of C_2H_2/CO values from 3.5 to 1.0 (pptv/ppbv). In comparing PEM-WB with PEM-WA, the smaller decrease in CH_4 for a given C_2H_2/CO value in PEM-WB may be indicative of the smaller biogenic CH_4 production expected during winter. The larger fractional changes for C_2H_6 compared with CH_4 for the same range of C_2H_2/CO are similar to PEM-WA and are expected based on C_2H_6's shorter lifetime (~2 months versus ~8 years). The same statement can be made for other NMHCs relative to CH_4. The relative amount of processing for C_3H_8 and C_6H_6 is in reasonably good agreement with their comparable lifetimes of ~1 month. The lower mixing ratios of C_6H_6 observed during PEM-WB compared with those of PEM-WA are interesting. They could be the result of lower C_6H_6 emissions, but there is no other evidence supporting this notion.

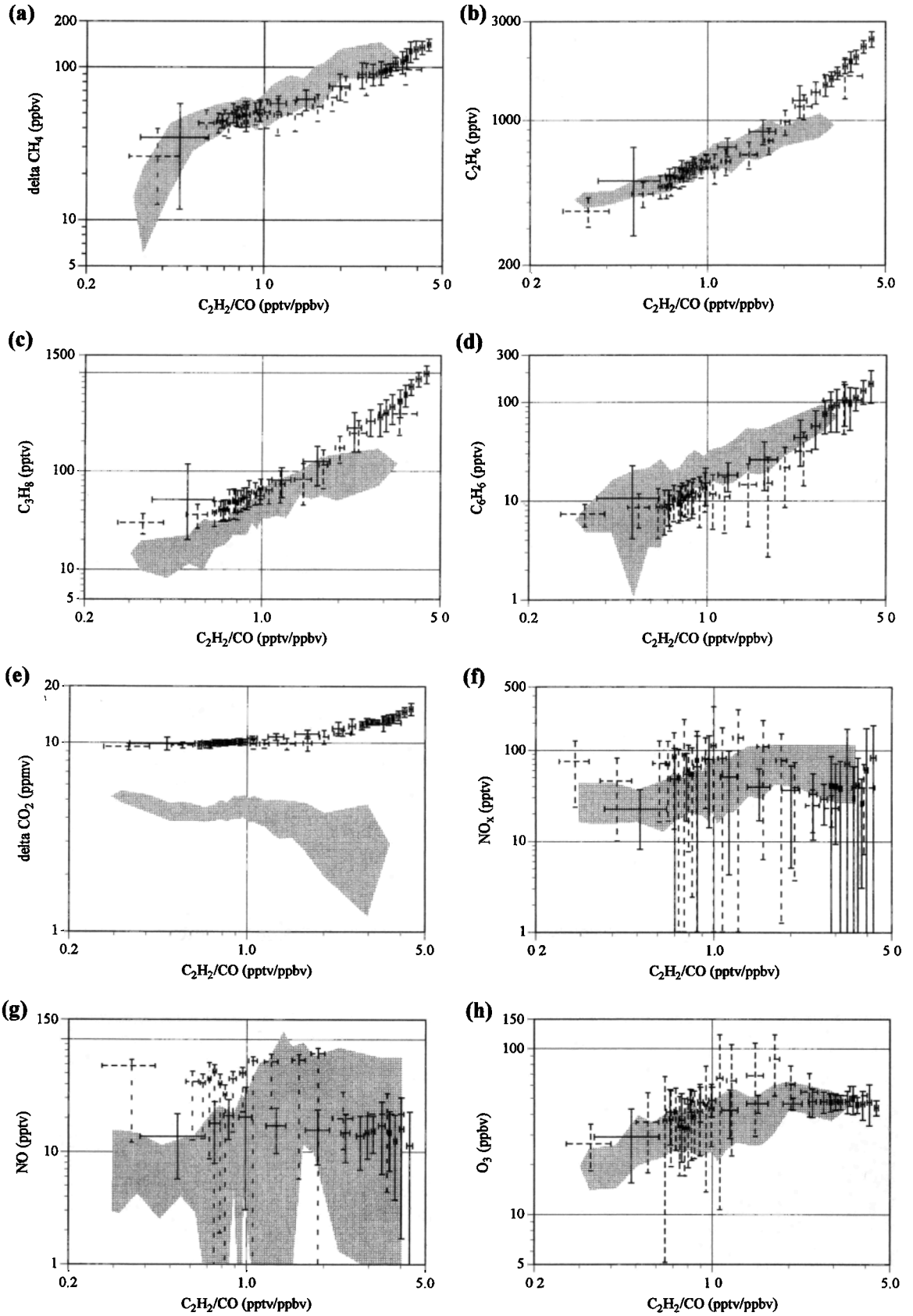

Figure 2. Graphs of the data similar to Figure 1 for PEM-West B flights 6-20 for selected trace gases versus the ratio C_2H_2/CO, separated into two altitude regimes (2–7 km, denoted by solid crosses, and 7–12 km, denoted by dashed crosses, for (a) ΔCH_4, (b) C_2H_6, (c) C_3H_8, (d) C_6H_6, (e) ΔCO_2, (f) NO_x, (g) NO, and (h) O_3, where NO_x is calculated by taking the Georgia Tech laser-induced fluorescence (LIF) instrument NO and adding model-calculated NO_2. The shaded regions represent the entire PEM-West A data set above 2 km within $\pm 1\sigma$. In order to highlight the variability, ΔCH_4 and ΔCO_2 are shown by subtracting 1.68 ppmv and 350 ppmv from the absolute mixing ratios of CH_4 and CO_2, respectively.

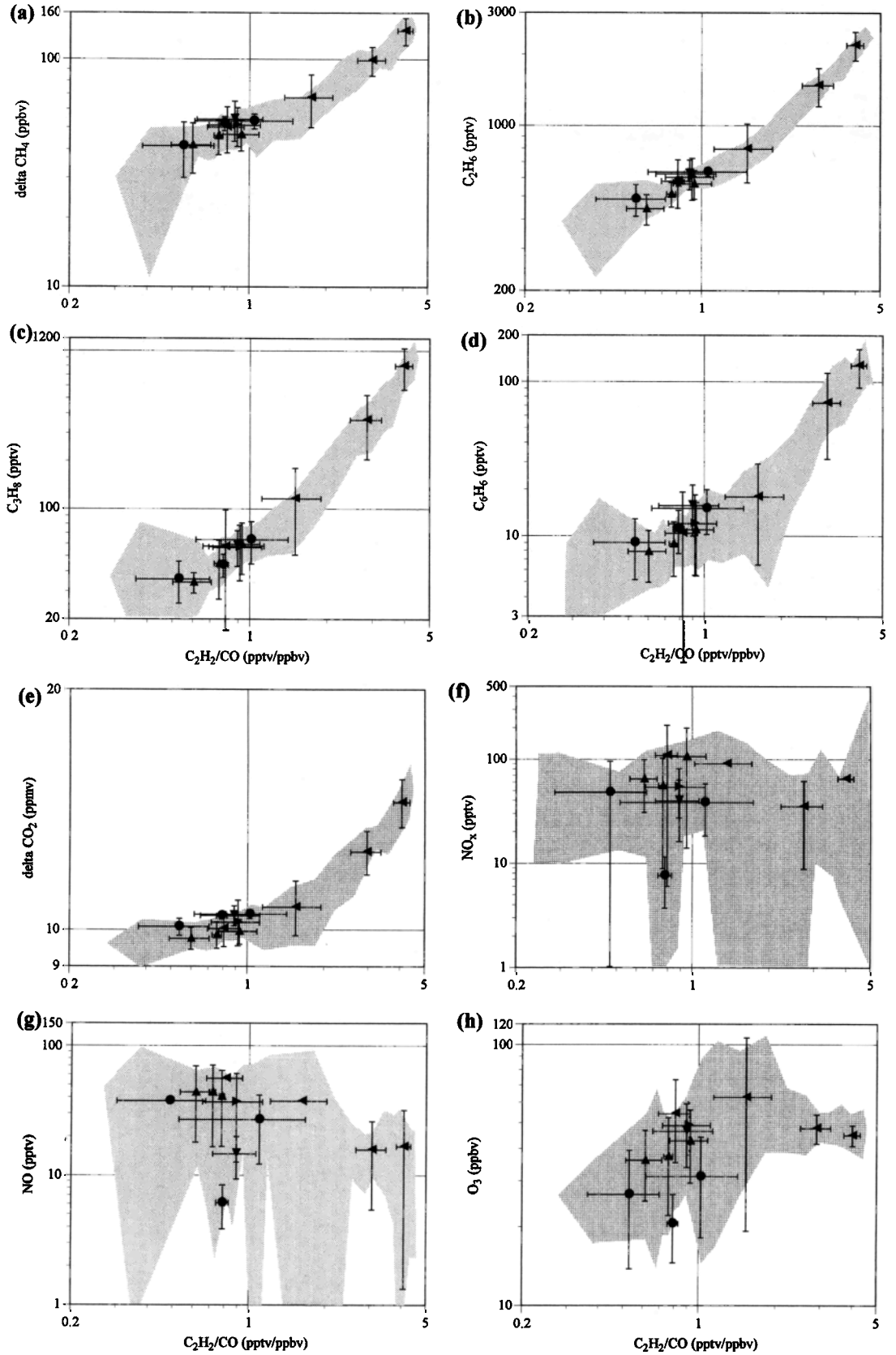

Figure 3. Relationships between the degree of atmospheric processing indicated by the ratio C_2H_2/CO and large-scale trajectory-based air mass classification schemes of *Talbot et al.* [1997] for (a) ΔCH_4, (b) C_2H_6, (c) C_3H_8, (d) C_6H_6, (e) ΔCO_2, (f) NO_x, (g) NO, and (h) O_3. The shaded regions represent the entire PEM-West B data set above 2 km within $\pm 1\sigma$. The symbols denote the origin of the air mass as follows: north continental air less than 2 days from the Asian coast, solid left pointing triangles; north continental air greater than 2 days from the Asian coast, solid right pointing triangles, south continental air less than 2 days from the Asian cost, solid upward pointing triangles; south continental air greater than 2 days from the Asian coast, downward pointing triangles; and marine air, solid circles.

Several important conclusions can be drawn from these trends. First, the maximum NMHC levels and C_2H_2/CO are larger for PEM-WB than for PEM-WA, resulting in an expanded scale of less processed air for this chemically based air mass classification scheme in PEM-WB relative to PEM-WA. This clearly indicates that on average the trace gases emitted from the continent during winter underwent less atmospheric processing. Second, there are a significantly greater number of observations (proportional to the number of crosses in Figures 2a–2h) with C_2H_2/CO values >2 than the number of observations with C_2H_2/CO values <2 in the 2- to 7-km altitude bin, while the opposite is true for the 7- to 12-km bin. This implies that the air masses in the lower troposphere that originated from the continent are less processed by the atmospheric chemistry and mixing than those in the upper troposphere. This is consistent with the fact that the pollutants in major continental outflows were, in general, limited to below 6 km during PEM-WB [*Hoell et al.*, 1997]. In contrast, during PEM-WA, *Smyth et al.* [1996] showed that air masses in the 2- to 7-km bin were more processed by the atmospheric chemistry and mixing than air masses in the 7- to 12-km bin. This is because more active convective activities over the continent during PEM-WA transported more pollutants to the upper troposphere and then to the Pacific basin by the westerlies [*Blake et al.*, 1996; *Liu et al.*, 1996].

In sharp contrast to the results obtained from PEM-WA, CO_2 mixing ratios during PEM-WB exhibit a significant covariance with respect to C_2H_2/CO that is similar to the NMHCs (Figure 2e). As shown by the shaded region, during autumn (PEM-WA), CO_2 uptake by plants resulted in smaller CO_2 values at larger C_2H_2/CO ratios (i.e., there was more continental influence), whereas in more atmospherically processed air masses (i.e., those with less continental influence) CO_2 mixing ratios were larger [*Smyth et al.*, 1996; *Anderson et al.*, 1996]. The covariance of CO_2 with respect to C_2H_2/CO during PEM-WB is expected, since during the winter months plant uptake of CO_2 should be smaller than the emissions from fossil fuel [e.g., *Fung et al.*, 1983]. The PEM-WA results suggested the Asian continent acted as a sink for CO_2 in the autumn, while the winter results clearly show it as a major source.

Figures 2f and 2g illustrate that NO and NO_x (NO_2 is calculated from NO by assuming photochemical equilibrium, as described by *Davis et al.* [1996]) mixing ratios exhibit a substantial (~20 pptv) enhancement from PEM-WA to PEM-WB in the region of C_2H_2/CO values less than 2.0 pptv/ppbv, for which a substantial number of the data are from the low latitudes. The increase is particularly significant in the upper troposphere in regard to the production of O_3, as the absolute values of NO and NO_x mixing ratios are high. The enhancement of NO and NO_x in more processed air is most likely due to an increase in the lightning-generated NO. This was supported by the significant increase in lightning activities observed both on board the DC-8 and the Defense Meteorological Satellite (DMSP) during PEM-WB at low latitudes compared with those of PEM-WA [*Crawford et al.*, 1997a]. Further discussion on this important point will be given later.

Similarly, O_3 mixing ratios also increase with processing, however, only at high altitudes and above 1.0 on the atmospheric processing scale (i.e., the C_2H_2/CO scale). The O_3 mixing ratios are the largest between 1.0 and 2.0 on the atmospheric processing scale. This is the same region where NO and NO_x attain their maximums. Given the fact NO_x is usually the rate-limiting precursor of O_3 photochemical production, it is not surprising to find that high O_3 levels correlate with high concentrations of NO and NO_x. We note that relatively high levels of O_3 extend below C_2H_2/CO values less than 1.0 pptv/ppbv, again corresponding to relatively high values of NO and NO_x. This is consistent with the results of *Crawford et al.* [1997a] and S. C. Liu et al. (unpublished manuscript, 1999) that showed large production of O_3 when NO_x was high and a significant correlation of O_3 and NO_x at low latitudes, respectively.

4. Combination of C_2H_2/CO With Other Air Mass Classification Schemes

As stated in section 1, the chemical-based (C_2H_2/CO) scheme can provide a valuable independent tool for investigating the distributions and budgets of atmospheric trace species, as we have done in the previous section. More important, the chemical-based (C_2H_2/CO) scheme complements the back-trajectory and LIDAR air mass classification schemes extremely well, and thus the (C_2H_2/CO) scheme can be combined with the latter schemes to become a more powerful tool for analyzing and interpreting the observations. These combinations are carried out in the next two sections.

4.1. Combination of C_2H_2/CO With Back-Trajectory Scheme

Talbot et al. [1997] presented the chemical signatures of PEM-WB air masses that were classified based on the back-trajectory analysis of *Merrill et al.* [1997]. In a similar analysis for the PEM-WA study, the trajectory-based scheme of classifying air masses aided the interpretation of the results from the chemical-based (C_2H_2/CO) scheme. Such a comparison for PEM-WB should provide insight into some of the apparent differences in the atmospheric processing between the autumn and late winter–early spring in the western Pacific. Figures 3a–3h depict mean values for PEM-WB air masses classified as marine (solid circles), southern continental (upward and downward pointing triangles), and northern continental (left and right pointing triangles). For the marine case, back-trajectories indicated that the air masses had resided over the western Pacific for at least 5 days prior to interception. The continental cases were segregated by latitude (i.e., northern, >20°N, and southern, <20°N) as well as by the indicated air mass travel time from landfall, which led to groupings of less than 2 days travel time (solid left pointing triangles) and between 2 and 4 days travel time (solid right pointing triangles). As can be seen, those air masses that recently originated from northern Asia (i.e., <2 days and >20°N latitude) have enhanced average values for all of the compounds examined here as well as the largest average ratios of C_2H_2/CO.

For C_2H_2/CO values greater than approximately 1.5 pptv/ppbv, only the northern continental air masses with less than 2 days travel time appear to contribute significantly to the distributions of all compounds. This is in stark contrast to the air masses that originated from the southern continental region, where air masses with both less than and greater than 2 days travel time have mean compositions that are similar to those found in the marine classified air masses. Such a large difference was not observed in the PEM-WA study, in which average values of CH_4, C_2H_6, C_3H_8, and C_6H_6 for a given C_2H_2/CO ratio were nominally within approximately 10% regardless of whether the origin was from the southern or northern conti-

nental regions for the same travel time from the expected source region. This difference between PEM-WA and PEM-WB may be associated with an enhanced ventilation of the boundary layer as wintertime frontal passages swept out the northern continental region (i.e., enhanced continental outflow), which is reflected in the larger C_2H_2/CO ratios.

In the southern continental cases the inability to segregate travel time with respect to C_2H_2/CO may indicate that, on average, tracer inputs occurred much farther upwind than 2 days and may imply only a weak coupling to eastern Asia's boundary layer, which we have chosen as a reference point for establishing air mass travel times. In the southern continental air masses, C_2H_2/CO values range from 0.5 to 1.0 (pptv/ppbv) and are close to values for the greater than 2-day northern continental air masses. This suggests that the southern continental air masses are more representative of air that has not been significantly impacted by this region's surface sources and that the input of compounds from sources upwind of eastern Asia accounts for a large part of the observed mixing ratios of NMHCs and other compounds in southern continental and greater than 2-day northern continental air. The tropical air with relatively low NMHC and CO mixing ratios is also partially responsible for the lack of higher mixing ratios of NMHCs in the southern continental cases because back-trajectories also show equatorial air circulated over the southern continent back over the Pacific [*Merrill et al.*, 1997].

Instantaneous ozone formation and destruction rates for PEM-WB from model results [*Crawford et al.*, 1997b] are similarly distributed across the range of C_2H_2/CO values from 0.8 to 4.0 pptv/ppbv. The model results suggest the northern continental air masses above 1.0 on the C_2H_2/CO scale contribute to the net formation of ozone. This is expected, as the NMHC mixing ratios discussed earlier are generally high and the NO_x mixing ratios are also relatively high. The net O_3 formation rates at 2.0 and 4.0 pptv/ppbv of C_2H_2/CO were approximately 3×10^5 and 5×10^5 molecules cm^{-3} s^{-1}, respectively. Even at the lowest C_2H_2/CO ratio, the marine cases are expected to be net ozone producers, at least in the upper troposphere. In fact, one of the highest net O_3 production regions observed over the northern Pacific during PEM-WB is apparently for the southern continental air masses less than 2 days from the continent ($\sim 6 \times 10^5$ molecules cm^{-3} s^{-1}).

It is also important to note that the older continental air masses based on the C_2H_2/CO ($\sim$0.9 pptv/ppbv) and trajectory methods (2 to 4 day) do not differ significantly from less processed air ($\sim$2.0 pptv/ppbv) in terms of net O_3 production. The reason can be seen in Figures 3f and 3g, which show similar amounts of NO_x and NO in the 2- to 4-day and less than 2-day-old air masses. The levels of NO_x in the C_2H_2/CO range of 2–5 pptv/ppbv are approximately 60 pptv, where only a modest reduction (5–10 pptv NO_x) from this is observed around a C_2H_2/CO value of about 0.9 pptv/ppbv. The same relationship exists for the two marine aggregate means at 1.2 and 0.47 pptv/ppbv on the C_2H_2/CO scale. In this marine air, net O_3 production is similar to that observed for the continental air masses with similar mixing ratios of NO_x. However, the marine aggregate in the middle of the marine air mass distribution has very low NO_x ($\sim$9 pptv) and a near-zero or negative net O_3 production, i.e., a loss. This strong dependence of net O_3 production on NO_x mixing ratios highlights the importance of identifying the in situ sources of NO_x, which are suspected to be the primary sources.

The components of atmospheric processing (i.e., mixing and chemistry) should be seasonally dependent, and assessing how that dependence manifests itself in our C_2H_2/CO chemical coordinate can provide insight into each process's relative contribution. For example, comparing the average C_2H_2/CO value (approximately 2.0 pptv/ppbv) for the northern continental air masses with travel times from land of less than 2 days (solid left pointing arrow) to the average (approximately 0.8 pptv/ppbv) for air masses with 2- to 4-day travel times (solid right pointing arrow) can yield an estimate of the equivalent degree of atmospheric processing on the time coordinate of OH's reactions with C_2H_2 and CO (i.e., the corresponding time for reaction with OH to remove an equivalent amount of the compound, hereinafter referred to as the "OH-process time"). On the basis of a diurnal average OH concentration of 1×10^6 molecules cm^{-3}, greater than 20 days are needed for OH-processing alone to produce the average difference between the C_2H_2/CO values in the less-than-2-day and 2- to 4-day northern continental air masses. This time is approximately tenfold larger than the time difference based on the trajectories. This implies that during two additional days of travel, the equivalent of 20 days of OH-driven atmospheric processing occurred. In addition, taking a source emission value of approximately 9 pptv/ppbv [*Blake et al.*, 1996] results in approximately 40 days being required for OH-processing alone to reduce the ratio to the values observed in the northern continental less-than-2 day air masses. This result is of magnitude similar to that found in our previous PEM-WA analysis.

Uncertainties involved in the estimates above include both the initial emission ratio, which probably varies with season, and the estimated OH concentration. The emission ratio was derived from several flights into urban areas during PEM-WA [*Blake et al.*, 1996]. An overestimate of the emission ratio would result in an overestimate of the OH-process time. However, this estimate can have reasonable bounds placed on it. For instance, from the range of the C_2H_2/CO values in Figures 3a–3h, the lower limit for the emission ratio value must be at least 5.0 (pptv/ppbv) and yields a minimum OH-process time of approximately 23 days. The diurnal average OH concentration most likely does not vary by more than a factor of 2, suggesting a 10- to 30-day OH processing time.

The PEM-WA analysis concluded that a primary role of photochemistry was to control the "background" mixing ratios of the trace gases and that the resulting background mixing ratios were inversely proportional to their sinks. This results in an increased "apparent" importance of atmospheric mixing contributing disproportionately to the changes in observed levels. This notion is reconfirmed in the analysis of PEM-WB observations.

4.2. Combined C_2H_2/CO With LIDAR Scheme

E. V. Browell et al. (unpublished data, 1998) classified the air masses encountered during PEM-WB by using criteria based on LIDAR observations of O_3 and aerosol levels in the troposphere in conjunction with an analysis of potential vorticity. Using this approach, they distinguished seven types of air as characteristic of the air masses encountered during the PEM-WB study. They defined these (see Figures 4a–4h) as high ozone plumes (designated by solid squares), background plumes (downward pointing triangles), continental convective outflows (crosses), marine convective outflows (solid squares with crosses), clean Pacific (solid circles), background (solid diamonds), and stratospherically influenced (upward pointing triangle).

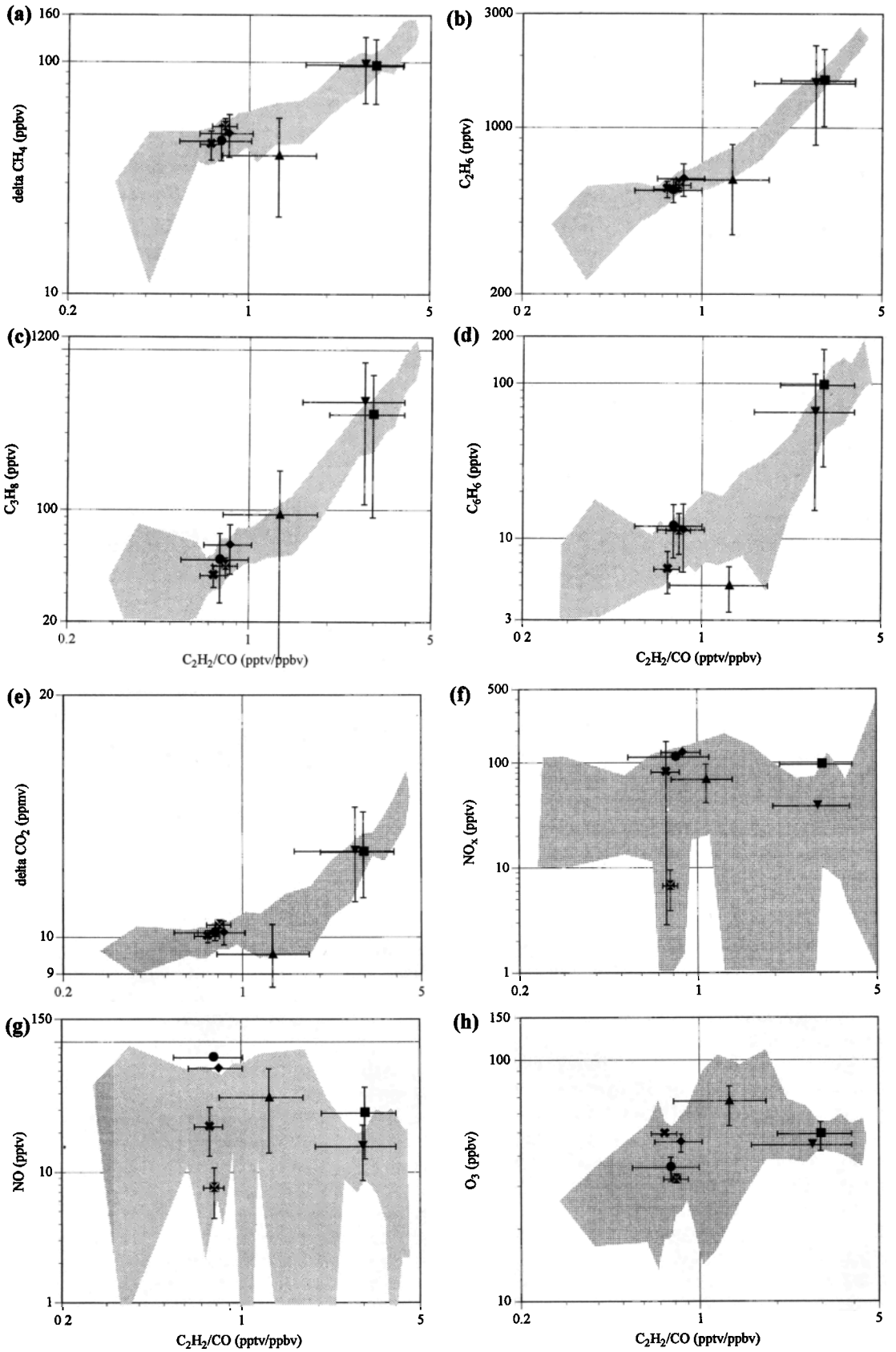

Figure 4. Relationships between the degree of atmospheric processing indicated by the ratio C_2H_2/CO and LIDAR ozone- and aerosol-based air mass classification schemes of E. V. Browell et al. (unpublished data, 1998), for high-ozone plumes (solid squares); continental-convective (crosses); background plumes (downward pointing triangles); oceanic-convective (crosses with solid squares); clean Pacific (solid circles); background (solid diamonds); and stratospherically influenced (upward pointing triangle) types of air masses. Shown are (a) ΔCH_4, (b) C_2H_6, (c) C_3H_8, (d) C_6H_6, (e) ΔCO_2, (f) NO_x, (g) NO, and (h) O_3. The shaded regions represent the entire PEM-West B data set above 2 km within $\pm 1\sigma$.

Several aspects of the distributions depicted in Figures 4a–4h might be expected based on our discussions thus far. In particular, the two plume categories do lie at the high end of C_2H_2/CO values, which is consistent with the expectation of "fresher" or less processed inputs of surface emissions. Enhanced levels of CO_2, CH_4, and NMHCs in these air masses are also evidence of the expectation. However, NO_x and O_3 are only slightly enhanced in these plumes when compared with the other air mass categories (except the stratospheric air) or even with generally more processed marine air (i.e., air having smaller values of C_2H_2/CO). This is partly due to the high O_3 in the stratospheric air. Another reason is that the high NO_x levels in the background and Pacific air masses at low latitudes are very conducive to production of O_3. Also, as might be expected, the air classified as having been stratospherically influenced is seen to have significantly greater O_3 levels but smaller levels of CO_2, CH_4, and most NMHCs for this air mass category's corresponding average value of C_2H_2/CO. The level of C_2H_2/CO may be deceiving for the stratospheric cases because the low mixing ratios of both C_2H_2 and CO in stratospheric air may result in a relatively high C_2H_2/CO ratio. However, the anomalously enhanced levels of C_3H_8 also suggest that even though these air masses exhibit signs of stratospheric inputs, they also exhibit signs of having been impacted significantly by tropospheric air. In particular, the tropospheric air may primarily originate from middle- and higher-latitude regions where wintertime C_3H_8 utilization may be disproportionately enhanced [*Blake et al.*, 1997]. With respect to NO_x the stratosphere does not appear to play a large role in the NO_x enhancements because the ratio of NO_x to total reactive nitrogen is relatively small in the stratospheric air [*Kotamarthi et al.*, 1997].

For most of the hydrocarbon compounds depicted, there is also little discernable difference between the background and convective outflow categories. The exceptions to this are the reduced levels of C_6H_6 and C_3H_8 in the continental convective category compared with the three other cases. These reduced levels of C_6H_6 and C_3H_8 may seem contrary to expectations for a continental category, but given the level of processing of these four LIDAR air mass types designated by the C_2H_2/CO scale, the variable signatures are expected. In fact, the low values are not inconsistent with the well-processed continental cases in the trajectory method as shown in Figures 2c and 2d. The C_2H_6 levels are attenuated for all except the highest C_2H_2/CO values for the same LIDAR cases [*Smyth et al.*, 1996] observed from PEM-WA, suggesting that continental influence of C_2H_6 is less for a given value of C_2H_2/CO during the winter.

The significant difference (approximately tenfold larger values) between NO_x levels in the continental and marine convective outflows may support *Crawford et al.*'s [1997a] contention that the lightning-generated NO_x from over continental regions can add a significant amount of NO_x to the upper troposphere over the western Pacific in comparison with the much weaker lightning rates from tropical marine deep convection [e.g., *Price and Rind*, 1994; *Goodman et al.*, 1988; *Goldenbaum and Dickerson*, 1993]. These enhanced NO_x levels may also be responsible for some of the O_3 enhancement in the continental convective category. The lack of discernable enhancement in O_3 between the plume categories is consistent with the slow midlatitude, late-winter O_3 production, and the continental convective outflow category may suggest that the plume category of air masses does not produce significantly more O_3 in comparison with the continental convective outflow air masses.

As discussed in sections 3 and 4.1, in situ sources may have also contributed significantly to the observed level of NO_x as evidenced by the anomalously enhanced levels of NO_x in the background air mass categories. This is further supported by the fact that NO_x levels do not appreciably decline with increases in the degree of atmospheric processing (compare Figure 2g for C_2H_2/CO ratios less than approximately 1 pptv/ppbv). Circumstantial evidence has been used to imply that most of this NO_x enhancement is due to lightning from westward tropical continental regions [*Crawford et al.*, 1997a]. However, the lack of such a large increase in the LIDAR continental convective classified air masses may also indicate that other in situ sources, perhaps from sources upwind of Asia, may be important. Another alternative explanation is that the intercepted continental convective outflows that were characterized by the LIDAR-based analysis represent the lower-altitude edges of the outflows and that the dominant NO_x input occurs at altitudes well above the DC-8 aircraft's 13-km ceiling altitude. In this situation the enhanced NO_x levels observed in the background categories may represent convective outflows that had subsided during their eastward or northward travel from upstream tropical continental regions, as suggested by *Davis et al.* [1996] and *Koch et al.* [1996]. Here the apparent seasonal difference between the PEM-WA and PEM-WB studies may be representative of a larger contribution from tropical deep convection north of the Intertropical Convergence Zone (ITCZ) during the late winter (see also discussion by *Crawford et al.* [1997a]). This type of mechanism may contribute significantly to the large increase in the LIDAR scheme's clean Pacific (P) and background (K) air mass categories which ranged from 5 to 20 pptv NO_x during the PEM-WA study and from 60 to 70 pptv NO_x in the PEM-WB study. Alternatively, enhanced recycling of NO_x can also not be ruled out as a possible consequence of the dramatically reduced upper tropospheric sulfate levels in PEM-WB.

4.3. Sources of NO_x and O_3 Production in the Tropics

As mentioned previously, the older continental air masses and portions of the marine air masses demonstrated no loss of ability to produce O_3 despite the evolution from high to low C_2H_2/CO values, which typically is associated with travel time from Asia. *Crawford et al.* [1997a] describes two typical scenarios, referred to as "high" and "low" NO_x regimes at low latitudes. The high NO_x regime displays mixing ratios of the order of 60–70 pptv at 8–10 km, in contrast to low NO_x air, where values are less than 10 pptv. In addition, by using a time-dependent box model, they have shown that the O_3 production is essentially proportional to the mixing ratio of NO_x. The median values of C_2H_2/CO for the low and high NO_x regimes discussed by *Crawford et al.* [1997a] are shown in Figure 5. This figure shows clearly that there is a lack of a dependence of NO_x levels on the C_2H_2/CO value. This means that the O_3 production is also independent of the value of C_2H_2/CO, consistent with earlier analysis. Furthermore, it is remarkable that there is no statistically meaningful difference in the altitude distribution of C_2H_2/CO. This is consistent with the fact that there were substantial convective activities over the tropics that led to efficient vertical transport (S. C. Liu et al., unpublished manuscript, 1999).

Figure 5 also shows that the values of C_2H_2/CO are relatively low for both high and low NO_x regimes. This again must be the

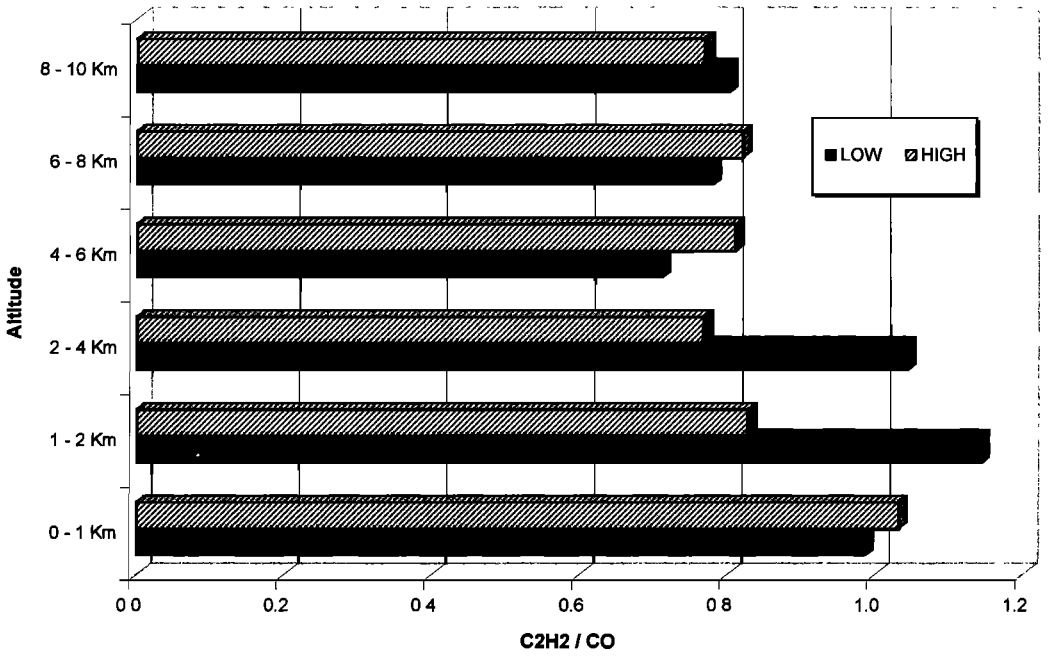

Figure 5. Vertical distribution of C_2H_2/CO median values for the indicated altitude ranges based on the "low" and "high" NO_x regimes from *Crawford et al.* [1997a] observed during PEM-West B.

result of substantial convective activity over the tropics, which is known to be an extremely effective mixing process. The C_2H_2/CO indicator shows that the air in both regimes is processed to a greater extent at higher altitudes (>4 km) than at lower altitudes. This is expected for convective transport of surface-emitted compounds. The difference along our atmospheric processing scale is negligibly small (i.e., 0.7 versus 0.8 pptv/ppbv) in the free troposphere between the high and low NO_x regimes, suggesting the air of both regimes is similarly processed once it reaches the higher altitudes. The difference in NO_x mixing ratios, however, indicates a dependence upon both the region where deep convection takes place and the resulting in situ source strength (i.e., lightning), as suggested by *Crawford et al.* [1997a]. The similarity in NO_x values between the northern (higher air traffic) and southern continental air masses together with the indications of a large seasonal shift may imply that aircraft emissions are not the dominant source. However, photochemical recycling cannot be ruled out as this in situ source of NO_x, as both could also exhibit a tendency to not correlate with surface emission tracers.

5. Summary

Analysis of the PEM-WB data set confirms that the chemical-based (C_2H_2/CO) scheme can not only provide a valuable independent tool for investigating the distributions and budgets of atmospheric trace species but also complement the back-trajectory and LIDAR air mass classification schemes. In addition, the analysis indicates that atmospheric mixing makes a large contribution to the total atmospheric processing of surface emissions into this region. This finding is consistent with that of PEM-WA and suggests that whereas chemistry is important for establishing the region's background mixing ratios, vertical and horizontal mixing (or dilution) processes provide the dominant mechanisms controlling postemission levels of trace species.

Certain important seasonal differences can be readily discerned by comparing PEM-WB with PEM-WA. There is a clear increase of continental outflow during winter/spring compared with autumn, as evident by the significant increase in both the absolute values of anthropogenic NMHCs and the C_2H_2/CO value during PEM-WB compared with PEM-WA. In addition, the relationship between the level of CO_2 and the C_2H_2/CO ratio changes drastically from PEM-WA to PEM-WB, showing the dominance by biological uptake during autumn and an anthropogenic source in late winter/early spring. Similarly, relative CH_4 mixing ratios exhibited the general depression that might be expected during the less biologically active period of late winter/early spring.

NO_x mixing ratios were significantly enhanced during PEM-WB when compared with PEM-WA, particularly in the upper troposphere's more atmospherically processed air masses. As a result, the O_3 production was substantially greater during PEM-WB. A lack of corresponding enhancements in surface emission tracers implies that in situ atmospheric sources are responsible for the enhanced upper tropospheric NO_x. The similarity in NO_x values between the northern (higher air traffic) and southern continental air masses together with the indications of a large seasonal shift suggests that aircraft emissions are not the dominant source. However, photochemical recycling cannot be ruled out as this in situ source of NO_x since it can also exhibit a tendency to not correlate with surface emission tracers. The most plausible explanation of the above results is provided by *Crawford et al.*'s [1997a] conclusion that lightning significantly contributed to NO_x in the western Pacific's tropical upper troposphere.

Acknowledgments. We extend our thanks to NASA (like PEM-WA) and to our staff at Georgia Tech: Deanna Doherty, Amy Tilghman, Kelly Fitzgerald, and Margaret Heuer. We also recognize the DAAC at NASA Langley for help in retrieving valuable data from PEM-WB.

References

Anderson, B. E., G. L. Gregory, J. E. Collins Jr., G. W. Sachse, T. J. Conway, and G. P. Whiting, Airborne observations of spatial and temporal variability of tropospheric carbon dioxide, *J. Geophys. Res.*, *101*, 1985–1997, 1996.

Blake, D. R., T. Chen, T. W. Smith Jr., C. J.-L. Wang, O. W. Wingenter, N. J. Blake, F. S. Rowland, and E. W. Mayer, Three-dimensional distribution of nonmethane hydrocarbons and halocarbons over the northwestern Pacific during the 1991 Pacific Exploratory Mission (PEM-West A), *J. Geophys. Res.*, *101*, 1763–1778, 1996.

Blake, N. J., D. R. Blake, T.-Y. Chen, J. E. Collins Jr., G. W. Sachse, B. E. Anderson, and F. S. Rowland, Distribution and seasonality of selected hydrocarbons and halocarbons over the western Pacific basin during PEM-West A and PEM-West B, *J. Geophys. Res.*, *102*, 28,315–28,331, 1997.

Browell, E. V., et al., Large-scale air mass characteristics observed over the western Pacific during summertime, *J. Geophys. Res.*, *101*, 1691–1712, 1996.

Crawford, J. H., et al., Implications of large-scale shifts in tropospheric NO_x levels in the remote tropical Pacific, *J. Geophys. Res.*, *102*, 28,447–28,468, 1997a.

Crawford, J. H., et al., An assessment of ozone photochemistry in the extratropical western North Pacific: Impact of continental outflow during the late winter/early spring, *J. Geophys. Res.*, *102*, 28,469–28,487, 1997b.

Davis, D. D., et al., Assessment of ozone photochemistry in the western North Pacific as inferred from PEM-West A observations during the fall 1991, *J. Geophys. Res.*, *101*, 2111–2134, 1996.

Fung, I., K. Prentice, E. Matthews, J. Lerner, and G. Russell, Three-dimensional tracer model study of atmospheric CO_2: Response to seasonal exchanges with the terrestrial biosphere, *J. Geophys. Res.*, *88*, 1281–1294, 1983.

Goldenbaum, G. C., and R. R. Dickerson, Nitric oxide production by lightning discharges, *J. Geophys. Res.*, *98*, 18,333–18,338, 1993.

Goodman, S. J., H. J. Christian, and W. D. Rust, A comparison of the optical pulse characteristics of intracloud and cloud-to-ground lightning as observed above clouds, *J. Appl. Meteorol.*, *27*, 1369–1381, 1988.

Gregory, G. L., A. S. Bachmeier, D. R. Blake, B. G. Heikes, D. C. Thornton, A. R. Bandy, J. D. Bradshaw, and Y. Kondo, Chemical signatures of aged Pacific marine air: Mixed layer and free troposphere as measured during PEM-West A, *J. Geophys. Res.*, *101*, 1727–1742, 1996.

Hoell, J. M. Jr., D. D. Davis, S. C. Liu, R. E. Newell, H. Akimoto, R. J. McNeal, and R. J. Bendura, The Pacific Exploratory Mission-West Phase B: February–March, 1994, *J. Geophys. Res.*, *102*, 28,223–28,239, 1997.

Koch, D. M., D. J. Jacob, and W. C. Graustein, Vertical transport of tropospheric aerosols as indicated by ^{7}Be and ^{210}Pb in a chemical tracer model, *J. Geophys. Res.*, *101*, 18,651–18,666, 1996.

Kotamarthi, V. R., J. M. Rodriguez, N. D. Sze, Y. Kondo, R. Pueschel, G. Ferry, J. Bradshaw, S. Sandholm, G. Gregory, D. Davis, and S. Liu, Evidence of heterogeneous chemistry on sulfate aerosols in stratospherically influenced air masses sampled during PEM-West B, *J. Geophys. Res.*, *102*, 28,425–28,436, 1997.

Liu, S. C., et al., A model study of tropospheric trace species during PEM-West A, *J. Geophys. Res.*, *101*, 2073–2085, 1996.

McKeen, S. A., and S. C. Liu, Hydrocarbon ratios and photochemical history of air masses, *Geophys. Res. Lett.*, *20*, 2363–2366, 1993.

McKeen, S. A., S. C. Liu, E.-Y. Hsie, X. Lin, J. D. Bradshaw, S. Smyth, G. L. Gregory, and D. R. Blake, Hydrocarbon ratios during PEM-West A: A model perspective, *J. Geophys. Res.*, *101*, 2087–2109, 1996.

Merrill, J. T., R. E. Newell, and A. S. Bachmeier, A meteorological overview for the Pacific Exploratory Mission-West Phase B, *J. Geophys. Res.*, *102*, 28,241–28,253, 1997.

Price, C., and D. Rind, Possible implications of global climate change on global lightning distributions and frequencies, *J. Geophys. Res.*, *99*, 10,823–10,831, 1994.

Sandholm, S. T., et al., Summertime tropospheric observations related to N_xO_y distributions and partitioning over Alaska: Arctic Boundary Layer Expedition 3A, *J. Geophys. Res.*, *97*, 16,481–16,509, 1992.

Sandholm, S. T., et al., Summertime partitioning and budget of NO_y compounds in the troposphere over Alaska and Canada: ABLE 3B, *J. Geophys. Res.*, *99*, 1837–1861, 1994.

Singh, H. B., and P. B. Zimmerman, Atmospheric distribution and sources of nonmethane hydrocarbons, in *Gaseous Pollutants: Characterization and Cycling*, edited by J. O. Nriaaagu, pp. 177–235, John Wiley, New York, 1992.

Smyth, S., et al., Comparison of free tropospheric western Pacific air mass classification schemes for the PEM-West A experiment, *J. Geophys. Res.*, *101*, 1743–1762, 1996.

Talbot, R., et al., Chemical characteristics of continental outflow from Asia to the troposphere over the western Pacific Ocean during September–October 1991: Results from PEM-West A, *J. Geophys. Res.*, *101*, 1713–1725, 1996.

Talbot, R., et al., Chemical characteristics of continental outflow from Asia to the troposphere over the western Pacific Ocean during February–March, 1994: Results from PEM-West B, *J. Geophys. Res.*, *102*, 28,255–28,274, 1997.

B. Anderson, E. Browell, J. Collins, M. Fenn, G. Gregory, and G. Sachse, NASA Langley Research Center, Mail Stop 472, Hampton, VA 23681.

S. Bachmeier, Department of Atmospheric, Oceanic and Space Science, University of Wisconsin, Madison, 1125 W. Dayton Street, Madison, WI 53706.

D. Blake and S. Rowland, Department of Chemistry, University of California at Irvine, Irvine, CA 92717.

J. Bradshaw, A. Kanvinde, S. Liu, W. Mitch, S. Sandholm, B. Shumaker, and S. Smyth, School of Earth and Atmospheric Sciences, Georgia Institute of Technology, Atlanta, GA 30332-0340.

S. McKeen, NOAA Aeronomy Laboratory, Mail Stop R/E/AL4, 325 Broadway, Boulder, CO 80303.

J. Merrill, Graduate School of Oceanography, Center for Atmospheric Chemistry Studies, University of Rhode Island, Narragansett, RI 02882-1197.

R. Talbot, Institute for the Study of Earth, Oceans, and Space, University of New Hampshire, Durham, NH 03820.

(Received May 14, 1998; revised February 4, 1999;
accepted February 19, 1999.)